ELSEVIER

Journal of Photochemistry and Photobiology A: Chemistry 139 (2001) 79–87

Journal of Photochemistry and Photobiology A:Chemistry

www.elsevier.nl/locate/jphotochem

Conformational control of photoinduced decarboxylation of simple aryl esters. Enhancement by templating effects in polyethylene films

Weiqiang Gu, David J. Abdallah, Richard G. Weiss*

Department of Chemistry, Georgetown University, Washington, DC 20057-1227, USA

Received 29 June 2000; received in revised form 2 November 2000; accepted 3 November 2000

Abstract

The photochemistry of phenyl and 1-naphthyl esters has been investigated in solutions and in polyethylene films. Enhancement of photodecarboxylation at the expense of the 'normal' photo-Fries processes when the irradiations are conducted in polyethylene films at subambient temperatures is attributed to a 'templating' effect imposed by the large solute molecules on the polymer chains that constitute their reaction cavities. Evidence for the conformation of the esters that promotes photodecarboxylation comes from quantum chemical calculations, single-crystal X-ray analyses, and additional interpretation of data in the literature. © 2001 Elsevier Science B.V. All rights reserved.

Keywords: Temperature effects; Photo-Fries; X-ray; Decarbonylation

1. Introduction

Many unimolecular photochemical transformations, such as the Norrish–Yang reaction [1], are known to be conformationally dependent at several points along their reaction coordinates [2]. As a result, some photoproducts are not observed or are obtained in very low yields when specific precursor conformations are present in negligible amounts.

Less well understood and studied are the conformationally-dependent photoreactions of aromatic esters. Photo-Fries rearrangements [3] (Eq. (1)) are the most commonly reported processes [4]. However, as early as 1965, Finnegan and Knutson [5] reported that UV irradiations in refluxing benzene produce low yields of decarboxylation products from esters with bulky substituents near the position of acylate attachment. Subsequent work showed a distinct preference for decarboxylation in non-hydroxylic solvents, but there was no obvious correlation with solvent polarity [6]. Based upon these observations and net retention of configuration in the decarboxylation photoproduct of an optically active ester whose center of chirality is at C2′, a concerted process (implying an excited singlet state reaction) from a conformation like that in Fig. 1a (as well as the need for bulky substituents to attain it) was suggested [7]. There have been other reports of photodecarboxylations from highly substituted aryl esters in the interim, but most [8] proceed with low yields also.[1] The degree of stereoselectivity could not be ascertained at the time of the experiments because the absolute rotation of the product was not known. Data now available [10,11] indicate that the decarboxylation was highly stereoselective if not stereospecific.

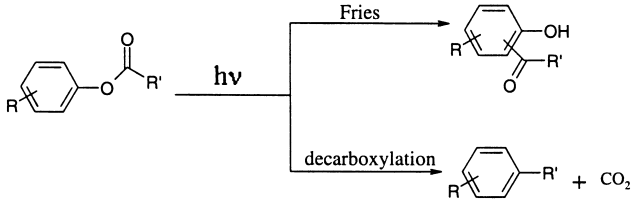

(1)

Very little effort seems to have been devoted to photodecarboxylations of simple aryl esters subsequently. The only example included in the reviews of Budac and Wan [12,13] on photodecarboxylation reactions involve cyclic

* Corresponding author. Tel.: +1-202-687-6013; fax: +1-202-687-6209.
E-mail address: weissr@gusun.georgetown.edu (R.G. Weiss).

[1] For an interesting example, see [9].

PII: S1010-6030(00)00411-1

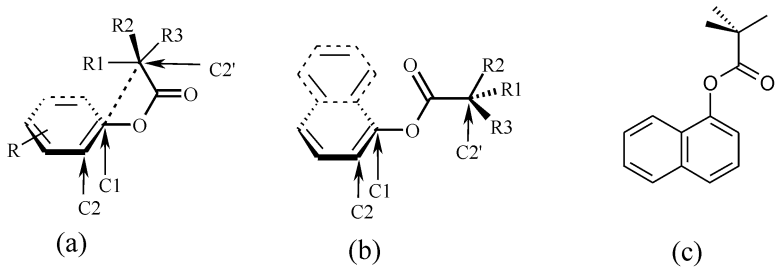

Fig. 1. (a) Conformation proposed by Finnegan and Knutson [5,7] leading to the transition state for concerted decarboxylation. The dashed line between C1 and C2′ indicates the new σ bond formed during the reaction and the (C2)-(C1)–O-C(=O) angle is 90°. (b) Approximate conformations in the single crystal structures of **2b** and **2c**. (c) Minimum energy conformation predicted for the first excited singlet state of **2c** by HF/6-31G calculations.

esters (i.e., lactones), and photodecarboxylations of only arylmethyl esters are covered in the review on the photochemistry of esters of carboxylic acids by Pincock [14]. Decarboxylations of benzylic acylates occur by a different mechanism [15]:

Here, we report that decarboxylation is a rather ubiquitous reaction that parallels photo-Fries rearrangements, but has different conformational requirements. Substituents on the aryl ring of the esters are not needed for loss of CO_2 and it is more efficient at *lower* temperatures in selected media. Specifically, we have exploited the 'templating' effect of reaction cavities in polyethylene films [16,17] to enhance the populations of conformations that favor decarboxylation (i.e., Fig. 1a) in excited singlet states, even though they are not favored energetically.

2. Experimental

The polyethylene films have been characterized previously [17,18]. High-density film (BHDPE, type ES-300 from Polialden Petroquimica, Brazil; 51% crystalline; density, 0.945 g cm^{-3}) and low-density film (NDLDPE, Sclair type from DuPont of Canada; 26% crystalline; density, 0.918 g cm^{-3}) were immersed sequentially in three chloroform aliquots during 1 week to remove additives, dried, and stored under a nitrogen atmosphere until used. Films were cold-stretched slowly by hand to ca. 4 (NDLDPE) or 5 (BHDPE) times their original length after being doped with an ester. BzN(**1**) and BzN(**2c**) were from Aldrich. All other photoproducts were either synthesized as described [16,17] or commercially available. Hexane, cyclohexane, and *t*-butyl alcohol were spectro or HPLC grade and were used as received.

Irradiations were conducted in closed tubes (quartz for **1**; Pyrex for **2**) under N_2 atmospheres. The radiation source for **1** was the ethanol-filtered output (to remove 189 nm) of an UV Products low-pressure Hg lamp (principally 254 nm). The source for **2** was a 450 W Hanovia medium-pressure Hg lamp with water and Pyrex filters (>300 nm). N_2-saturated hexane solutions contained 2 mM **1** or **2** and were analyzed by GC. Polyethylene films were doped with **1** or **2** in CH_2Cl_2, rubbed with a tissue soaked in hexane to remove surface-occluded molecules, dried under a stream of nitrogen, and irradiated. Photoproducts were extracted exhaustively from the films with CH_2Cl_2 and the extracts were combined for analyses [16,19].

Photoproducts were analyzed by GC on a Hewlett-Packard 5890 gas chromatograph equipped with a 15 m × 0.25 mm 0.25 μm Alltech DB-5 column, a flame-ionization detector, and a Hewlett-Packard 3393A integrator. They were identified by co-injections of reaction mixtures and authentic samples in GC analyses and by comparison of fragmentation patterns for those peaks and authentic samples during GC–MS analyses. Yields are based upon the amount of ester reacted and mass balances were >90%. Conversions were limited to <30% to avoid secondary photolyses.

All aspects of X-ray data collection were performed on a Siemens Smart CCD diffractometer using Mo Kα radiation ($\lambda = 0.71073$ Å) at 173(±2) K. The data were corrected for Lorentz and polarization effects, but not for absorption. The structure was solved using direct methods and refined against F^2 using the SHELXLT/PC v5.1 software suite and XSEED software. [2] All non-hydrogen atoms were refined anisotropically and the hydrogen atoms were included in calculated positions using a standard riding model and thermal parameters proportional to the non-hydrogen atom to which they are attached. Important crystallographic parameters and Ortep type drawings are included as Appendix A.

Calculations were performed at the PM3 level [20] for esters **2b** and **2c** in their electronic ground states and at the HF/6-31G level [21] for **2c** in its lowest excited singlet state. The initial geometry of **2c** was generated using Hyperchem with default bond lengths and angles. The starting conformations for geometry optimization in both ground and excited states were obtained by starting at (C1)-(O)–C-(C2′)

[2] Siemens Analytical X-ray Instruments, Madison, WI; L. Barbour, University of Missouri–Columbia, 1999.

dihedral angles of 0° or 180° and (C2)-(C1)–O-C(=O) equal to 90° (Fig. 1b).

3. Results and discussion

3.1. Structural considerations

Single-crystal X-ray diffraction analyses indicate that concerted decarboxylation of (±)-1-naphthyl-2-phenylpropanoate (**2b**) and 1-naphthyl acetate (**2c**) is not possible in their solid states, and no decarboxylation products were detected after prolonged irradiations. The conformations in the crystals are shown in Fig. 2 as Ortep drawings and as approximations in Fig. 1b; the distance between C2′ of the acylate chain and C1 of the naphthyl ring, 3.67 Å (**2b**) or 3.66 Å (**2c**), is too large for a concerted loss of CO_2 and C1–C2′ bond formation. (*R*) and (*S*) enantiomers of **2b** alternate within the crystalline lattice and have virtually mirror image conformations. Note that the phenyl rings are almost orthogonal to and are projected toward the naphthyls. See Appendix A for specific data concerning the crystal structures.

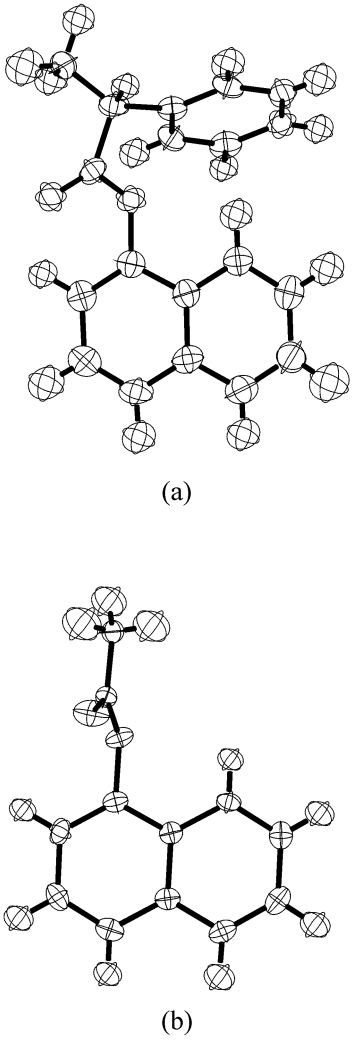

Fig. 2. ORTEP structures of: (a) 1-naphthyl-2-phenylpropanoate (**2b**); (b) 1-naphthyl acetate (**2c**) from analyses of single crystal X-ray diffraction data. The thermal ellipsoids represent 50% probability of electron density.

Table 1
(C1)-(O)–C-(C2′) (T1)[a] and (C2)-(C1)–O-C(=O) dihedral angles (T2)[a] from single crystal X-ray analyses and calculations on the globally and locally (in parentheses) minimized conformations

Compound	Electronic state	T1 (°)		T2 (°)	
		X-ray	Calculated	X-ray	Calculated
2b	S_0	162.8	0.1(175.9)	69.0	101.9(85.4)
2c	S_0	179.8	0.2(180.9)	88.8	87.3(84.2)
	S_1		180.0(3.3)		0(84.4)

[a] See Fig. 1b for the structure defining angles T1 and T2.

From semi-empirical calculations at the PM3 level, ground state conformations very near that favored for decarboxylation (Fig. 1a) are global minima. For **2b**, this conformation projects the phenyl ring *away* from the naphthyl ring. A local minimum, 1.3 kcal mol^{-1} above the global one, is like the conformation in Fig. 2a, but with the (C2)–O bond rotated by 180° (so that the phenyl ring is again projected *away* from naphthyl). A single point calculation of the crystal conformation of **2b** (Fig. 2a) predicts an energy 3.3 kcal mol^{-1} above the global minimum. A *local* minimum for **2c** like in Fig. 1b was 0.9 kcal mol^{-1} higher in energy. By contrast, ab initio calculations at the HF/6-31G level predict that Fig. 1c is the optimal geometry of the lowest energy excited singlet state of **2c**, and that Fig. 1a represents a shallow energy minimum, 6.5 kcal mol^{-1} higher in energy. The calculated and observed (C1)-O–C-(C2′) and (C2)-(C1)–O-C(=O) dihedral angles are presented in Table 1. Recent fluorescence excitation spectra of jet-cooled phenyl acetate and CIS/6-31 + G(D) calculations provide a (C2)-(C1)–O-C(=O) angle of 42.3° in the S_1 state [22]. Our ground-state calculations indicate that a relatively large mole fraction of our aryl esters prefer conformations conducive to decarboxylation in solution at (or below) room temperature. However, they change from such conformations after electronic excitation *unless internal or external steric constraints are applied.*

3.2. Irradiations in solutions

In solutions, irradiations of unsubstituted aromatic esters yield very small amounts of decarboxylation products. Hexane solutions of phenyl phenylacetate (**1**) and 1-naphthyl-2,2-dimethylphenylacetate (**2d**) at 22°C or 1-naphthyl phenylacetate (**2a**) and **2b** at 22 or 5°C produce ∼1% of the decarboxylation product (BzN), as well as large amounts of the expected photo-Fries and decarbonylation products (Scheme 1 [16,19]). Neither **2a** nor **2b** produced

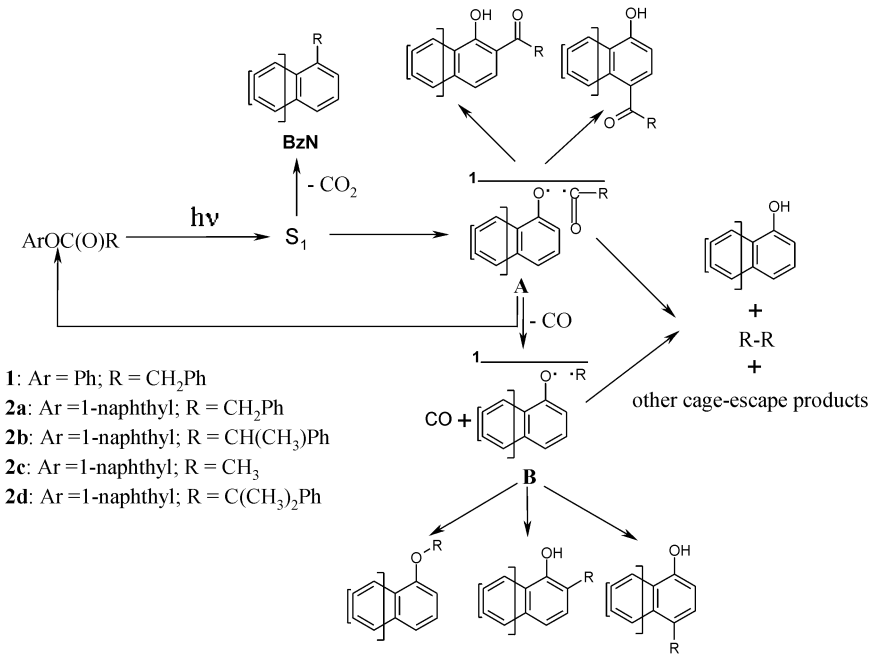

Scheme 1. Photoreactions of aryl esters [10,26].

a detectable amount of BzN(**2**) upon irradiation at room temperature in *t*-butyl alcohol, and ca. 1% of BzN(**2b**) was formed from **2b** in cyclohexane at both 10°C (liquid) and −8°C (dynamic plastic phase [23,24]). On these basis, the relative efficiency of the decarboxylation pathway depends somewhat upon solvent polarity [6], but not upon temperature (within the range investigated) or solvent phase when it is relatively mobile. Were decarboxylation a nonconcerted (triplet or singlet) process, some naphthalene should have been formed from **2**; we have not observed any upon irradiations in solution or in polyethylene films (vide infra). Also, we have demonstrated that these esters are not reactive in their lowest triplet states [16].

In addition to influencing the distribution of ground and excited state conformations, phenyl rings of the acyl parts of **1**, **2a**, **2b**, and **2d** also increase the rate of acyl radical decarbonylation [3] (leading to radical pair B; Scheme 1) and, therefore, decrease the return of the initial radical pair A to starting ester. As a result, less ester should react via the decarboxylation route and more should proceed through Fries-related pathways (if conformational differences are ignored). Although photo-Fries rearrangements of **2c** (lacking an acyl phenyl group) continue to dominate in hexane at room temperature, 9–10% yields of 1-methylnaphthalene (BzN(**2c**)) were obtained at low (<10%) conversions [27]! Conformational factors must be important.

3.3. Irradiations in polyethylene films

Selected esters that did not yield significant amounts of BzN in hexane were irradiated in unstretched and stretched polyethylene films at several temperatures to investigate whether their decarboxylation yields could be increased. These media afford reaction cavities [28] that are much less malleable than those of cyclohexane, even in its plastic phase. Furthermore, when the dopant molecules are larger than the hole free volumes of the native films, as is the case here [17], the reaction cavities are 'templated' by their guests [16,17,19]. Irradiations of **1** in unstretched low- or high-density polyethylene films at room temperature resulted in no detectable (<0.2%) BzN(**1**). However, in both stretched films, the yields of BzN(**1**) were ca. 2%.

Contrary to observations in isotropic solutions, irradiations of **2b** in polyethylene films show a dramatic general increase in BzN(**2b**) as temperature is lowered. From the data in Fig. 3, several empirical conclusions to be reached: (1) decarboxylation is enhanced in stretched films; (2) more decarbonylation product is formed in the polyethylene of higher density (and greater crystallinity); (3) reduced temperature generally aids decarboxylation in the constraining environments afforded by polyethylene films.

The increased yields of decarboxylation products at lower temperatures (Fig. 3A) may result from higher rates of CO_2 loss, lower rates of O–C(=O) lysis (i.e., less efficient

[3] Rates of decarbonylation for acetyl (gas phase) [25], phenylacetyl (isooctane) [26], 2-phenylpropanoyl (isooctane) [26], and 2-methyl-2-phenylpropanoyl (isooctane) [26] at 22°C are 0.15, 4.8×10^6, 4.0×10^7, and $1.5 \times 10^8\ s^{-1}$, respectively.

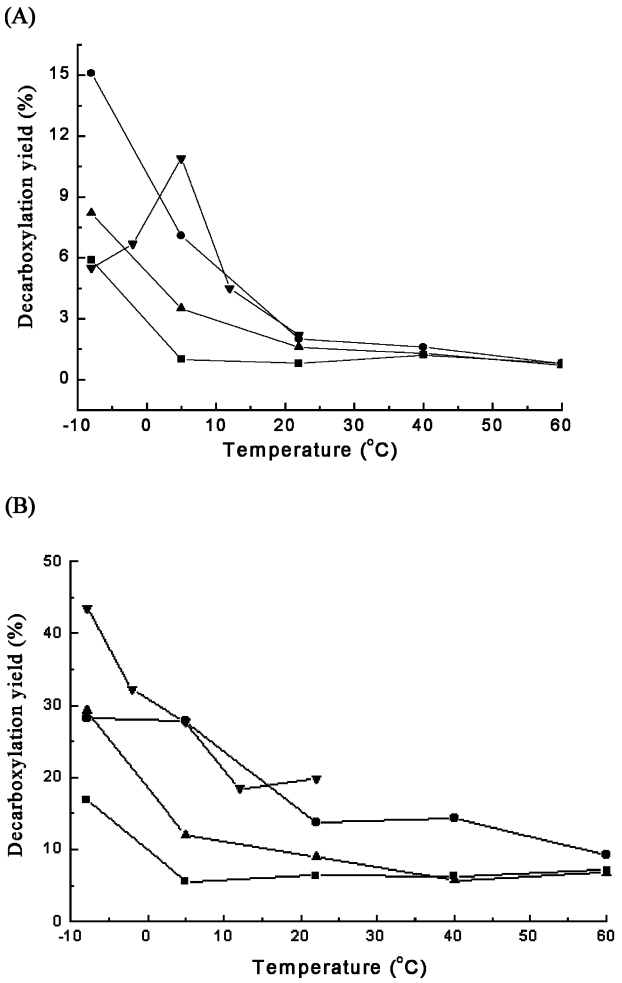

Fig. 3. Temperature dependence on relative decarboxylation (A) and decarbonylation (B) product yields from irradiations of **2b** in unstretched (u) and stretched (s) NDLDPE and BHDPE films: ■, NDLDPE (u); ●, NDLDPE (s); ▲, BHDPE (u); ▼, BHDPE (s).

formation of radical pair A in Scheme 1), more return of radical pair A to starting ester, or a combination of these factors. Stretching or cooling a polyethylene film stiffens the chains that constitute the "walls" of the reaction cavities [18,28–31]. As a result, motions of the singlet radical pairs A from their initial positions are attenuated, enhancing the probability that reformation of **1** or **2** will occur at the expense of photo-Fries rearrangements (that require much more radical pair reorganization within a reaction cavity) or decarbonylation (that requires prolongation of the radical pair lifetime [16,17]). Stiffer walls from lowering temperature or stretching a film should enhance decarbonylation processes (i.e., more products derived from radical pair B) relative to normal photo-Fries reactions (i.e., recombinations of radical pair A). The data in Fig. 3B are consistent with this hypothesis: the relative yields of decarbonylation products increase at lower temperatures or upon film stretching at one temperature.

At the same time, stiffer walls retain the imprint of the ground state ester for longer periods and, thereby, inhibit significant shape changes within the 10–20 ns lifetimes of the ester excited singlet state [16]. The quantum calculations, larger size of the guest molecules than the mean hole free volumes in the native films [17], and lack of dependence of BzN yields on temperature in 'normal' solutions suggest templating effects (inhibiting relaxation of excited state geometries from shapes like Fig. 1a) as the major contributor to the enhanced yields of decarboxylation products in polyethylene films at lower temperatures.

In this regard, the decrease in yields of BzN(**2b**) in stretched BHDPE below 5°C was not anticipated based on the trends in the other films. The absence of a similar decrease in decarboxylation yields in stretched NDLDPE or in decarbonylation yields in any of the films (Fig. 3B) indicates that cessation of β-relaxations, associated with side chain motions in the amorphous regions of the films (i.e., where esters **1** and **2** reside [18,32,33]) cannot explain the results in BHDPE; the onset of β-relaxations occurs in *low density* polyethylenes only near 0°C [34]. Regardless, lowering the temperature below ca. 0°C must have a more marked influence on the rigidity of the environments experienced by molecules of **2b** in the stretched high-density film. Additionally, the free volume in stretched BHDPE is smaller than in its unstretched form or in either unstretched or stretched NDLDPE at room temperature [17]. Lowering the temperature decreases the free volume even more [30,31] and, thereby, slows further the shape changes between conformations of electronically excited esters that are and are not amenable to concerted decarboxylation. The reason for the lack of a corresponding anomalous change in the decarbonylation yields may be due to the nature of the species involved: decarboxylation is a unimolecular, very rapid, concerted process, governed largely by ground-state conformations; decarbonylation products arise from protracted step-wise reactions of two vicinal species. The memory of ground state conformations is attenuated more the longer a radical pair lives, and the decarbonylation products derive from the mole fraction of radical pairs that are long-lived.

4. Conclusions

From the results reported here and previously [7,16,17], we conclude that conformations like that in Fig. 1a are, in fact, needed for photo-induced decarboxylation from excited singlet states. Although preferred in the ground states, such conformations are only local minima in the excited singlet states of simple aryl esters. Thus, either intramolecular steric effects (i.e., substituents placed on the aryl rings [5,7]) or intermolecular interactions (i.e., templating medium effects like those afforded by polyethylenes [17,19]) must be present to maintain conformations like that in Fig. 1a

for periods comparable to the excited singlet lifetimes (ca. 10–20 ns).

The yields of decarboxylation products have not been optimized with respect to ester structure, polyethylene type, or temperature. However, the trends are clear. Moreover, these results add an additional example [35,36] of how polyethylene is able to redirect the courses of photochemical reactions via templating effect.

Acknowledgements

We are grateful to the National Science Foundation and the Petroleum Research Foundation (administered by the American Chemical Society) for their support of this research. We thank Prof. V. Ramamurthy of Tulane University and Mr. Guangyu Sun (Georgetown University) for useful discussions.

Appendix A

X-ray structural analysis data for **2b** and **2c** (Tables 2–11). Crystal packing of **2b** showing the alternating arrangement of enantiomers. The naphthyl rings make an angle of ca. 45° with respect to the *bc* plane as shown in (Fig. 4).

Table 2
Crystal data and structure refinement for **2b**

Empirical formula	$C_{19}H_{16}O_2$
Formula weight	276.32
Temperature	173(2) K
Wavelength	0.71073 Å
Crystal system	Monoclinic
Space group	P2(1)/c
Unit cell dimensions	$a = 5.78100(10)$ Å, $\alpha = 90°$; $b = 15.8995(4)$ Å, $\beta = 95.1650(10)°$; $c = 15.9578(4)$ Å, $\gamma = 90°$
Volume, Z	1460.81(6) Å^3, 4
Density (calculated)	1.256 g cm^{-3}
Absorption coefficient	0.080 mm^{-1}
$F(0\,0\,0)$	584
Crystal size	0.52 mm × 0.22 mm × 0.22 mm
Theta range for data collection	1.81–28.24°
Limiting indices	$-7 \le h \le 7$, $-21 \le k \le 21$, $-21 \le l \le 21$
Reflections collected	16103
Independent reflections	3534 [R(int) = 0.0454]
Absorption correction	None
Refinement method	Full-matrix least-squares on F^2
Data/restraints/parameters	3534/0/255
Goodness-of-fit on F^2	0.992
Final R indices [$I > 2\sigma(I)$]	R1 = 0.0636, wR2 = 0.1691
R indices (all data)	R1 = 0.1047, wR2 = 0.2047
Extinction coefficient	0.002(3)
Largest diff. peak and hole	0.455 and −0.254e Å^{-3}

Table 3
Atomic coordinates (×10^4) and equivalent isotropic displacement parameters (Å^2 × 10^3) for **2b**. U(eq) is defined as one-third of the trace of the orthogonalized U^{ij} tensor

	x	y	z	U(eq)
O(1)	−1673(2)	5689(1)	3431(1)	51(1)
C(1)	−1291(3)	6476(1)	4969(1)	39(1)
O(2)	595(2)	6302(1)	4495(1)	42(1)
C(2)	−2611(4)	5849(1)	5267(1)	44(1)
C(3)	−4469(4)	6061(1)	5748(1)	49(1)
C(4)	−4953(4)	6882(2)	5908(1)	48(1)
C(5)	−3601(4)	7541(1)	5608(1)	44(1)
C(6)	−4062(4)	8402(2)	5756(2)	56(1)
C(7)	−2717(5)	9029(2)	5464(2)	63(1)
C(8)	−844(5)	8825(1)	4999(2)	60(1)
C(9)	−313(4)	8000(1)	4836(1)	48(1)
C(10)	−1688(3)	7343(1)	5135(1)	39(1)
C(11)	172(3)	5980(1)	3700(1)	39(1)
C(12)	2303(3)	6093(1)	3226(1)	42(1)
C(13)	2407(3)	7029(1)	3006(1)	39(1)
C(14)	545(3)	7419(1)	2542(1)	43(1)
C(15)	563(4)	8282(1)	2398(1)	46(1)
C(16)	2453(4)	8767(1)	2709(1)	47(1)
C(17)	4333(4)	8384(1)	3155(1)	47(1)
C(18)	4307(4)	7520(1)	3298(1)	44(1)
C(19)	2265(5)	5514(1)	2462(2)	52(1)

Table 4
Bond lengths (Å) and angles (°) for **2b**[a]

O(1)–C(11)	1.205(2)
C(1)–C(2)	1.368(3)
C(1)–O(2)	1.409(2)
C(1)–C(10)	1.426(3)
O(2)–C(11)	1.370(2)
C(2)–C(3)	1.415(3)
C(3)–C(4)	1.364(3)
C(4)–C(5)	1.417(3)
C(5)–C(6)	1.419(3)
C(5)–C(10)	1.429(3)
C(6)–C(7)	1.370(4)
C(7)–C(8)	1.405(4)
C(8)–C(9)	1.377(3)
C(9)–C(10)	1.422(3)
C(11)–C(12)	1.513(3)
C(12)–C(19)	1.526(3)
C(12)–C(13)	1.530(3)
C(13)–C(18)	1.394(3)
C(13)–C(14)	1.397(3)
C(14)–C(15)	1.391(3)
C(15)–C(16)	1.392(3)
C(16)–C(17)	1.386(3)
C(17)–C(18)	1.392(3)
C(2)–C(1)–O(2)	121.8(2)
C(2)–C(1)–C(10)	122.4(2)
O(2)–C(1)–C(10)	115.8(2)
C(11)–O(2)–C(1)	119.22(14)
C(1)–C(2)–C(3)	119.3(2)
C(4)–C(3)–C(2)	120.6(2)
C(3)–C(4)–C(5)	121.0(2)
C(4)–C(5)–C(6)	122.7(2)
C(4)–C(5)–C(10)	119.5(2)
C(6)–C(5)–C(10)	117.8(2)
C(7)–C(6)–C(5)	121.6(2
C(6)–C(7)–C(8)	119.9(2)

Table 4 (*Continued*)

C(9)–C(8)–C(7)	121.0(2)
C(8)–C(9)–C(10)	119.7(2)
C(9)–C(10)–C(1)	123.0(2)
C(9)–C(10)–C(5)	119.8(2)
C(1)–C(10)–C(5)	117.2(2)
O(1)–C(11)–O(2)	123.5(2)
O(1)–C(11)–C(12)	127.0(2)
O(2)–C(11)–C(12)	109.4(2)
C(11)–C(12)–C(19)	111.9(2)
C(11)–C(12)–C(13)	106.3(2)
C(19)–C(12)–C(13)	113.7(2)
C(18)–C(13)–C(14)	118.3(2)
C(18)–C(13)–C(12)	121.0(2)
C(14)–C(13)–C(12)	120.6(2)
C(15)–C(14)–C(13)	120.6(2)
C(14)–C(15)–C(16)	120.3(2)
C(17)–C(16)–C(15)	119.6(2)
C(16)–C(17)–C(18)	119.9(2)
C(17)–C(18)–C(13)	121.2(2)

[a] Symmetry transformations used to generate equivalent atoms.

Table 5
Anisotropic displacement parameters ($Å^2 \times 10^3$) for **2b**. The anisotropic displacement factor exponent takes the form: $-2\pi^2[h^2a^{*2}U^{11} + \cdots + 2hka^*b^*U^{12}]$

	U^{11}	U^{22}	U^{33}	U^{23}	U^{13}	U^{12}
O(1)	45(1)	60(1)	47(1)	−7(1)	5(1)	−8(1)
C(1)	36(1)	47(1)	33(1)	0(1)	1(1)	0(1)
O(2)	37(1)	49(1)	41(1)	−3(1)	3(1)	1(1)
C(2)	45(1)	45(1)	40(1)	2(1)	0(1)	−2(1)
C(3)	48(1)	59(1)	38(1)	5(1)	1(1)	−5(1)
C(4)	44(1)	65(1)	35(1)	0(1)	4(1)	0(1)
C(5)	42(1)	54(1)	34(1)	−3(1)	0(1)	5(1)
C(6)	52(1)	64(2)	51(1)	−12(1)	5(1)	10(1)
C(7)	69(2)	49(1)	70(2)	−11(1)	5(1)	4(1)
C(8)	63(2)	45(1)	72(2)	−4(1)	11(1)	−2(1)
C(9)	48(1)	47(1)	48(1)	−3(1)	6(1)	−4(1)
C(10)	37(1)	45(1)	34(1)	−2(1)	−2(1)	2(1)
C(11)	43(1)	36(1)	39(1)	2(1)	4(1)	4(1)
C(12)	39(1)	43(1)	43(1)	4(1)	4(1)	4(1)
C(13)	39(1)	43(1)	36(1)	0(1)	6(1)	3(1)
C(14)	39(1)	45(1)	44(1)	−1(1)	0(1)	0(1)
C(15)	44(1)	48(1)	45(1)	4(1)	3(1)	7(1)
C(16)	56(1)	39(1)	46(1)	1(1)	10(1)	2(1)
C(17)	45(1)	50(1)	48(1)	−4(1)	4(1)	−7(1)
C(18)	37(1)	52(1)	42(1)	4(1)	2(1)	1(1)
C(19)	61(2)	43(1)	55(1)	−2(1)	20(1)	2(1)

Table 6
Hydrogen coordinates ($\times 10^4$) and isotropic displacement parameters ($Å^2 \times 10^3$) for **2b**

	x	y	z	U(eq)
H(2)	−2314(34)	5243(14)	5129(13)	43(5)
H(3)	−5422(43)	5567(17)	5955(17)	68(7)
H(4)	−6200(44)	7025(15)	6276(16)	58(6)
H(6)	−5339(41)	8544(15)	6089(16)	58(7)
H(7)	−3176(48)	9652(20)	5586(18)	84(9)
H(8)	142(42)	9307(16)	4768(16)	61(7)
H(9)	1050(42)	7842(14)	4516(15)	55(6)
H(12)	3693(37)	5962(13)	3589(14)	41(5)

Table 6 (*Continued*)

	x	y	z	U(eq)
H(14)	−771(39)	7112(13)	2309(14)	48(6)
H(15)	−798(36)	8537(13)	2102(13)	42(5)
H(16)	2442(34)	9362(14)	2612(14)	45(6)
H(17)	5598(43)	8698(15)	3395(15)	57(7)
H(18)	5639(43)	7238(14)	3603(15)	57(7)
H	964(45)	5637(16)	2029(17)	58(7)
H	3810(43)	5579(14)	2184(15)	53(6)
H	2086(46)	4906(20)	2638(18)	77(8)

Table 7
Crystal data and structure refinement for **2c**

Empirical formula	$C_{12}H_{10}O_2$
Formula weight	186.20
Temperature	173(2) K
Wavelength	0.71073 Å
Crystal system	Orthorhombic
Space group	P2(1)2(1)2(1)
Unit cell dimensions	$a = 5.400$ Å, $\alpha = 90°$; $b = 9.78220(10)$ Å, $\beta = 90°$; $c = 17.963$ Å, $\gamma = 90°$
Volume, Z	948.930(10) $Å^3$,4
Density (calculated)	1.303 g cm^{-3}
Absorption coefficient	0.088 mm^{-1}
F(0 0 0)	392
Crystal size	0.48 mm × 0.22 mm × 0.22 mm
Theta range for data collection	2.27–28.28°
Limiting indices	$-7 \le h \le 7$, $-12 \le k \le 12$, $-23 \le l \le 23$
Reflections collected	10809
Independent reflections	2323 [R(int) = 0.0272]
Absorption correction	None
Refinement method	Full-matrix least-squares on F^2
Data/restraints/parameters	2323/0/167
Goodness-of-fit on F^2	1.051
Final R indices [$I > 2\sigma(I)$]	R1 = 0.0304, wR2 = 0.0745
R indices (all data)	R1 = 0.0343, wR2 = 0.0764
Absolute structure parameter	0.8(10)
Largest diff. peak and hole	0.146 and −0.207e $Å^{-3}$

Table 8
Atomic coordinates ($\times 10^4$) and equivalent isotropic displacement parameters ($Å^2 \times 10^3$) for **2c**. U(eq) is defined as one-third of the trace of the orthogonalized U^{ij} tensor

	x	y	z	U(eq)
O(2)	−169(2)	5965(1)	5763(1)	29(1)
C(12)	−1743(2)	6481(1)	6991(1)	23(1)
C(7)	−3476(2)	7215(1)	7434(1)	26(1)
C(6)	−5373(2)	7986(1)	7083(1)	31(1)
C(11)	134(2)	5700(1)	7340(1)	27(1)
C(3)	−2003(2)	6580(1)	6207(1)	25(1)
C(8)	−3256(2)	7144(1)	8220(1)	32(1)
C(4)	−3840(2)	7315(1)	5877(1)	31(1)
O(1)	−2469(2)	4066(1)	5638(1)	45(1)
C(9)	−1418(3)	6386(1)	8543(1)	35(1)
C(10)	287(2)	5657(1)	8102(1)	33(1)
C(5)	−5556(2)	8023(1)	6325(1)	33(1)
C(1)	1524(3)	4203(1)	5045(1)	34(1)
C(2)	−608(2)	4679(1)	5504(1)	26(1)

Table 9
Bond lengths (Å) and angles (°) for **2c**[a]

O(2)–C(2)	1.3614(13)
O(2)–C(3)	1.4072(14)
C(12)–C(11)	1.416(2)
C(12)–C(3)	1.419(2)
C(12)–C(7)	1.423(2)
C(7)–C(8)	1.419(2)
C(7)–C(6)	1.420(2)
C(6)–C(5)	1.364(2)
C(11)–C(10)	1.372(2)
C(3)–C(4)	1.360(2)
C(8)–C(9)	1.368(2)
C(4)–C(5)	1.410(2)
O(1)–C(2)	1.195(2)
C(9)–C(10)	1.408(2)
C(1)–C(2)	1.490(2)
C(2)–O(2)–C(3)	117.79(9)
C(11)–C(12)–C(3)	123.19(10)
C(11)–C(12)–C(7)	119.72(10)
C(3)–C(12)–C(7)	117.09(10)
C(8)–C(7)–C(6)	121.93(11)
C(8)–C(7)–C(12)	118.46(11)
C(6)–C(7)–C(12)	119.62(10)
C(5)–C(6)–C(7)	120.63(11)
C(10)–C(11)–C(12)	120.07(11)
C(4)–C(3)–O(2)	119.49(10)
C(4)–C(3)–C(12)	122.72(11)
O(2)–C(3)–C(12)	117.64(10)
C(9)–C(8)–C(7)	120.61(12)
C(3)–C(4)–C(5)	119.36(11)
C(8)–C(9)–C(10)	120.72(11)
C(11)–C(10)–C(9)	120.42(12)
C(6)–C(5)–C(4)	120.56(12)
O(1)–C(2)–O(2)	122.79(11)
O(1)–C(2)–C(1)	127.14(11)
O(2)–C(2)–C(1)	110.07(10)

[a] Symmetry transformations used to generate equivalent atoms.

Table 10
Anisotropic displacement parameters ($Å^2 \times 10^3$) for **2c**. The anisotropic displacement factor exponent takes the form: $-2\pi^2[h^2a^{*2}U^{11} + \cdots + 2hka^*b^*U^{12}]$

	U^{11}	U^{22}	U^{33}	U^{23}	U^{13}	U^{12}
O(2)	31(1)	29(1)	27(1)	−5(1)	8(1)	−4(1)
C(12)	22(1)	21(1)	26(1)	−1(1)	2(1)	−4(1)
C(7)	24(1)	25(1)	29(1)	−3(1)	4(1)	−3(1)
C(6)	27(1)	26(1)	40(1)	−2(1)	5(1)	2(1)
C(11)	25(1)	27(1)	30(1)	−1(1)	2(1)	0(1)
C(3)	27(1)	22(1)	26(1)	−2(1)	4(1)	−3(1)
C(8)	34(1)	34(1)	29(1)	−5(1)	7(1)	−4(1)
C(4)	37(1)	28(1)	28(1)	2(1)	−2(1)	−2(1)
O(1)	35(1)	35(1)	66(1)	−14(1)	9(1)	−7(1)
C(9)	42(1)	40(1)	24(1)	−1(1)	0(1)	−6(1)
C(10)	31(1)	37(1)	31(1)	3(1)	−5(1)	−1(1)
C(5)	30(1)	28(1)	42(1)	4(1)	−4(1)	3(1)
C(1)	37(1)	34(1)	30(1)	−2(1)	5(1)	7(1)
C(2)	28(1)	27(1)	23(1)	−1(1)	−2(1)	1(1)

Table 11
Hydrogen coordinates ($\times 10^4$) and isotropic displacement parameters ($Å^2 \times 10^3$) for **2c**

	x	*y*	*z*	*U*(eq)
H	1609(31)	5147(16)	8324(9)	42(4)
H	1250(29)	5223(15)	7048(8)	33(4)
H	−4000(28)	7367(15)	5346(9)	36(4)
H	−1324(30)	6354(17)	9092(9)	45(4)
H	−6525(30)	8491(16)	7383(8)	39(4)
H	−6844(31)	8546(17)	6096(8)	43(4)
H	3027(41)	4327(22)	5304(11)	68(6)
H	1349(35)	3233(20)	4907(10)	61(5)
H	1639(41)	4748(23)	4610(12)	76(6)
H	−4512(33)	7632(16)	8523(9)	47(4)

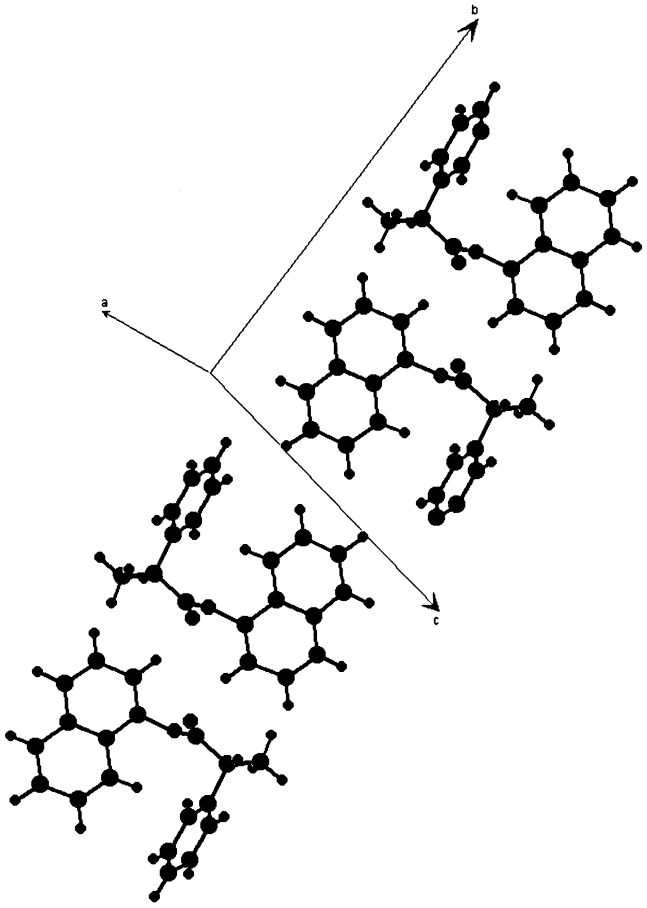

Fig. 4. Crystal packing of **2b** showing the alternating arrangement of enantiomers. The napthyl rings make an angle of ca. 45° with respect to the *bc* plane as shown above.

References

[1] P.J. Wagner, in: W.M. Horspool, P.-S. Song (Eds.), CRC Handbook of Photochemistry and Photobiology, CRC Press, Boca Raton, FL, 1995 (Chapter 38).
[2] V. Ramamurthy (Ed.), Photochemistry in Organized and Constrained Media, VCH, New York, 1991.
[3] J.C. Anderson, C.B. Reese, Proc. Chem. Soc. London (1960) 217.

[4] M.A. Miranda, in: W.M. Horspool, P.-S. Song (Eds.), CRC Handbook of Photochemistry and Photobiology, CRC Press, Boca Raton, FL, 1995 (Chapter 47) and references cited therein.
[5] R.A. Finnegan, D. Knutson, Chem. Ind. (1965) 1837.
[6] R.A. Finnegan, D. Knutson, Tetrahedron Lett. (1968) 3429.
[7] R.A. Finnegan, D. Knutson, J. Am. Chem. Soc. 89 (1967) 1970.
[8] T. Mori, T. Wada, Y. Inoue, Org. Lett. 2 (2000) 3401.
[9] H. Ishii, F. Sekiguchi, T. Ishikawa, Tetrahedron 37 (1981) 285.
[10] J. Kenyon, H. Phillips, V.P. Pitman, J. Chem. Soc. (1935) 1072.
[11] G. Bettoni, C. Cellucci, F. Berardi, J. Heterocycl. Chem. 17 (1980) 603.
[12] D. Budac, P. Wan, J. Photochem. Photobiol. A 67 (1992) 135.
[13] P. Wan, D. Budac, in: W.M. Horspool, P.-S. Song (Eds.), CRC Handbook of Organic Photochemistry and Photobiology, CRC Press, Boca Raton, FL, 1994 (Chapter 31).
[14] J.A. Pincock, in: W.M. Horspool, P.-S. Song (Eds.), CRC Handbook of Organic Photochemistry and Photobiology, CRC Press, Boca Raton, FL, 1994 (Chapter 32).
[15] S.A. Fleming, J.A. Pincock, in: V. Ramamurthy, K. Schanze (Eds.), Molecular and Supramolecular Photochemistry: Organic Molecular Photochemistry, Vol. 3, Marcel Dekker, New York, 1999, p. 211.
[16] W. Gu, R.G. Weiss, Tetrahedron 56 (2000) 6913.
[17] W. Gu, A.J. Hill, X. Wang, C. Cui, R.G. Weiss, Macromolecules 33 (2000) 7801.
[18] O.E. Zimerman, C. Cui, X. Wang, T.D.Z. Atvars, R.G. Weiss, Polymer 39 (1998) 1177.
[19] W. Gu, M. Warrier, V. Ramamurthy, R.G. Weiss, J. Am. Chem. Soc. 121 (1999) 9467.
[20] "Gaussian 94" Program by M.J. Frisch, G.W. Trucks, H.B. Schlegel, P.M.W. Gill, B.G. Johnson, M.A. Robb, J.R. Cheeseman, T. Keith, G.A. Petersson, J.A. Montgomery, K. Raghavachari, M.A. Al-Laham, V.G. Zakrzewski, J.V. Ortiz, J.B. Foresman, J. Cioslowski, B.B. Stefanov, A. Nanayakkara, M. Challacombe, C.Y. Peng, P.Y. Ayala, W. Chen, M.W. Wong, J.L. Andres, E.S. Replogle, R. Gomperts, R.L. Martin, D.J. Fox, J.S. Binkley, D.J. Defrees, J. Baker, J.P. Stewart, M. Head-Gordon, C. Gonzalez, J.A. Pople, Gaussian, Inc., Pittsburgh, PA, 1995.
[21] "Gaussian 98" Program by M.J. Frisch, G.W. Trucks, H.B. Schlegel, G.E. Scuseria, M.A. Robb, J.R. Cheeseman, V.G. Zakrzewski, J.A. Montgomery Jr., R.E. Stratmann, J.C. Burant, S. Dapprich, J.M. Millam, A.D. Daniels, K.N. Kudin, M.C. Strain, O. Farkas, J. Tomasi, V. Barone, M. Cossi, R. Cammi, B. Mennucci, C. Pomelli, C. Adamo, S. Clifford, J. Ochterski, G.A. Petersson, P.Y. Ayala, Q. Cui, K. Morokuma, D.K. Malick, A.D. Rabuck, K. Raghavachari, J.B. Foresman, J. Cioslowski, J.V. Ortiz, B.B. Stefanov, G. Liu, A. Liashenko, P. Piskorz, I. Komaromi, R. Gomperts, R.L. Martin, D.J. Fox, T. Keith, M.A. Al-Laham, C.Y. Peng, A. Nanayakkara, C. Gonzalez, M. Challacombe, P.M.W. Gill, B. Johnson, W. Chen, M.W. Wong, J.L. Andres, C. Gonzalez, M. Head-Gordon, E.S. Replogle, J.A. Pople, Gaussian, Inc., Pittsburgh, PA, 1998.
[22] T. Egawa, T. Yamada, S. Konaka, Chem. Phys. Lett. 324 (2000) 260.
[23] W.J. Dunning (Ed.), The Plastically Crystalline Phase, Wiley, New York, 1979.
[24] K.J. McGrath, R.G. Weiss, Langmuir 13 (1997) 4474.
[25] L. Lunazzi, K.U. Ingold, J.C. Scaiano, J. Phys. Chem. 87 (1983) 529, and references cited therein.
[26] N.J. Turro, I.R. Gould, B.H. Baretz, J. Phys. Chem. 87 (1983) 531.
[27] C. Cui, X. Wang, R.G. Weiss, J. Org. Chem. 61 (1996) 1962.
[28] R.G. Weiss, V. Ramamurthy, G.S. Hammond, Acc. Chem. Res. 26 (1993) 530.
[29] C. Serna, J.Ch. Abbe, G. Duplatre, Phys. Stat. Sol. A 115 (1989) 389.
[30] D. Lin, S.J. Wang, J. Phys. Condens. Mat. 4 (1992) 3331.
[31] M.V. Prooijen, H.H. Jorch, J.R. Stevens, A. Rudin, Polymer 40 (1999) 5111.
[32] B. Wunderlich, Macromolecular Physics, Vol. I, Academic Press, New York, 1974.
[33] P.J. Phillips, Chem. Rev. 90 (1990) 425, and references therein.
[34] D.W. Hadley, in: I.M. Ward (Ed.), Structure and Properties of Oriented Polymers, Wiley, New York, 1975 (Chapter 9).
[35] V. Ramesh, R.G. Weiss, Macromolecules 19 (1986) 1486.
[36] C.-H. Tung, Z.-Y. Yuan, L.-Z. Wu, R.G. Weiss, J. Org. Chem. 64 (1999) 5156, and references cited therein.